Leveraging Antenna Side-lobe Information for Expedited Neighbor Discovery in Directional Terahertz Communication Networks

Qing Xia and Josep Miquel Jornet

Department of Electrical Engineering
University at Buffalo, The State University of New York
Buffalo, New York 14260, USA
E-mail: {qingxia, jmjornet}@buffalo.edu

Abstract— **Terahertz (THz)-band (0.1-10 THz) communication is envisioned as a potentially key technology to satisfy the need for much higher wireless data rates. The THz-band provides a huge transmission bandwidth, which ranges from hundreds of GHz up to a few THz. Nevertheless, this bandwidth comes at the cost of a very high pass loss, and, as a result, highly directional antennas are needed simultaneously in transmission and reception to establish a communication link beyond a few meters. In directional communication networks, efficient neighbor discovery is needed to overcome the deafness problem. Existing neighbor discovery protocols for lower frequency bands cannot be directly utilized, because they do not capture the peculiarities of the THz band or the need to support multi Giga-bit-per-second and even Tera-bit-per-second links. In this paper, a neighbor discovery protocol for THz-band communication networks that leverages the directional antenna side-lobe information is presented. More specifically, the full antenna radiation pattern is utilized to detect a series of effective signals and map them to a universal detection standard and expedite the neighbor discovery process. A mathematical framework is developed to compare the neighbor discovery protocols with and without the antenna side-lobe information, and numerical results are provided to illustrate the performance of the proposed neighbor discovery protocol in terms of total time needed to complete the discovery process.**

I. Introduction

The way in which our society creates, shares and consumes information has lead to a drastic increase in wireless data traffic. Not only there are more devices connected to the internet, but wireless data rates are much higher too. In particular, wireless data rates have grown 18-fold over the past 5 years [1] and are approaching the capacity of the wired communication systems. Following this trend, wireless Terabits-per-second (Tbps) links are expected to become a reality within the next five to ten years. In this context, Terahertz (THz)-band (0.1-10 THz) communication is envisioned as a key technology to satisfy the demand for such very high data-rates [2], [3].

The THz band provides wireless communication with an unprecedentedly large bandwidth, but this comes at the expense of a very high propagation loss [4], [5]. At THz frequencies, the attenuation that a propagating Electronic Magnetic (EM) wave suffers is mainly caused by the spreading loss and the molecular absorption loss. Resulting from the latter, the available bandwidth at THz frequencies changes significantly with transmission distance. For distances of up to one meter, the THz channel acts as a multi-THz window. However, as the transmission distance increases, the strength and width of the absorption lines increase, splitting the THz band in multiple multi-GHz transmission windows.

In light of the limited power of THz transceivers (from tens of microWatts [6] to tens of milliWatts [7]), highly Directional Antennas (DAs) are needed simultaneously on both transmitter and receiver to overcome the very high propagation loss and to establish communication links beyond a few meters. Directional communications face many challenges across the protocol stack. At the link layer, the deafness problem caused by applying highly DAs requests more feasible design for synchronization and medium access control (MAC). For example, in [8], we presented a receiver-initiated MAC protocol for THz communication that relied on the use of highly DAs. In the proposed solution, transmitters point their antennas toward the intended receivers, whereas receivers announce their availabilities to receive data while sweeping the space in discrete steps. We analytically and numerically showed that this protocol can support multi-Gbps throughputs, with minimal packet loss probability. Nevertheless, this protocol assumes that the transmitters know the relative location of their intended receivers. For this, neighbor discovery becomes of critical importance.

To the best of our knowledge, no neighbor discovery protocol has been developed for THz-band communication networks. Existing solutions for millimeter (mm)-wave (mm-wave) communication (30-300 GHz) cannot be directly reused. By considering that one of the communication node-pair equipped with an omnidirectional antenna and the other node with a directional antenna, the mm-wave communication technology, unfortunately, is insufficient to overcome the much higher propagation loss in THz-band communication networks. In this case, new neighbor discovery protocols, which capture the unique peculiarities of THz-band communication networks, are needed.

In this paper, we propose a neighbor discovery protocol for THz-band communication networks, which captures the aforementioned peculiarities. More specifically, the protocol

is built upon the aforementioned synchronization and MAC protocol based on high-speed turning DAs [8]. When the neighbor discovery process is triggered, a node periodically announces its presence while turning its DA in discrete steps. Under the assumption that the DA has only one main beam, we consider that two nodes can only find each other if they are exactly aligned and facing, which leads to very long neighbor discovery time. To overcome this problem, we suggest to leverage the presence of side-lobes. Indeed, as opposed to existing systems in which antenna side-lobes are either ignored or minimized, we utilize the full antenna radiation pattern with side-lobes to expedite the network discovery process, during which we map the effectively received signal to the universal detection standard. We analytically and numerically show that the neighbor discovery time can be significantly reduced. Compared with utilizing the ideal antenna model without side lobes, the analysis with the full antenna radiation pattern is more complex as it requires us to take into account also the interference [9]–[12] caused by the side-lobes. Nevertheless, the results are more accurate and expectedly closer to the real scenario.

The remainder of the paper is organized as follows. In Sec. II, we describe the network topology, the antenna array, and correspondingly, the received signal power strength. In Sec. III, we develop the proposed neighbor discovery protocol with side-lobes. In Sec. IV, we mathematically compare the performance between the neighbor discovery protocols with and without side-lobe information. In Sec. V, we provide the numerical results, and we conclude the paper in Sec. VI.

II. System Model

In this section, we describe the system model, including the network topology and the antenna model, based on which the received signal power is derived.

A. Network Topology

In this paper, we focus on one-hop neighbor discovery. To discover farther neighbors, the receiver can update its neighbor table based on the relayed neighbors' information from its closer neighbors.

As illustrated in Fig. 1, the discovering node is marked as RX. The one hop coverage area A of RX can be calculated as:

$$A = \pi R^2, \tag{1}$$

where R refers to the maximum radius of A, which is determined by the transmission power of each node.

All one-hop neighbors of RX, marked as TXs, are randomly distributed in A, following a Poisson distribution with node density λ_A. Thus, the total number of TXs is given by:
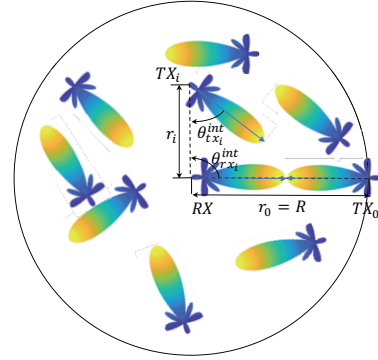
$$N_t = A\lambda_A. \tag{2}$$

Fig. 1: Network topology

B. Antenna Model

We consider all nodes are operating in the same elevation plane, i.e., the elevation beam angle ϕ of all antennas are zero. Further, each node is equipped with a time-delay antenna array. The normalized power gain pattern for an $N \times N$-elements planar array, in which each individual element is placed $\frac{\lambda}{2}$ apart, is calculated as [13]:

$$g(\theta) = \frac{1}{N^2} \frac{\sin^2\left(\frac{N}{2}\pi \sin\theta\right)}{\sin^2\left(\frac{1}{2}\pi \sin\theta\right)}, \tag{3}$$

which represents the practical DA gains including the side-lobes. The 2D radiation pattern of a 10×10-elements planar array is shown in Fig. 2 as a reference.
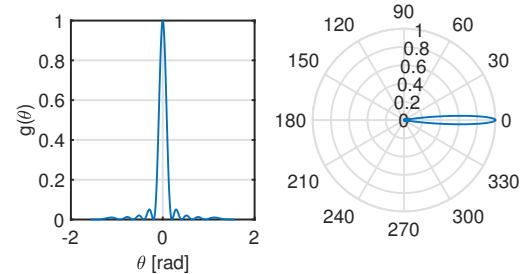

Fig. 2: Radiation pattern of 10×10-elements planar array

With the turning property of DAs in both transmitters and receivers, the received signal power at RX can be expressed as a function of the initial DA angles at the transmitter and the receiver, θ_{tx}^{int} and θ_{rx}^{int}, respectively, the discovering time t and frequency f:

$$P_{rx}(r, \theta_{tx}^{int}, \theta_{rx}^{int}, t, f) = \int_B S_{tx}(f) G_{max}^2(f) g(\theta_{tx}^{int} + \omega_{tx}t)$$
$$g(\theta_{rx}^{int} + \omega_{rx}t) \frac{c^2}{(4\pi f r)^2} e^{-K_{abs}(f)r} df, \tag{4}$$

where S_{tx} represents the power spectrum density of the transmitted signal, B refers to the $3\ dB$ bandwidth. ω_{tx} and ω_{rx} denote different antenna turning speeds of transmitter and receiver respectively. r is the distance between transmitter and receiver given that $r \leq R$. G_{max} denotes the maximum power pattern of the antennas and K_{abs} stands for the molecular absorption coefficient, both of them are functions of frequency

f. In order to simplify (4), we consider both the maximum power pattern of antenna and the molecular absorption loss to be constants over the operation $3\ dB$ frequency band, thus:

$$P_{rx}(r, \theta_{tx}^{int}, \theta_{rx}^{int}, t) = \gamma g(\theta_{tx}^{int} + \omega_{tx}t)g(\theta_{rx}^{int} + \omega_{rx}t)r^{-2}e^{-Kr},$$
(5)

where K is a constant and stands for $K_{abs}(f_0)$, f_0 denotes the central frequency of the $3\ dB$ frequency band, and constant $\gamma = P_{tx}G_{max}^2(f_0)\frac{c^2}{16\pi^2 f_0^2}$, where P_{tx} represents the transmitted signal power.

III. NEIGHBOR DISCOVERY WITH SIDE-LOBE INFORMATION

In this section, we derive the design logic of the proposed neighbor discovery protocol with side-lobe information. To fast and efficiently detect the direction of the received signal source with a series of continuous signal samples, the data patterns are specifically illustrated, and the mapping process between the received signal samples and the potential directions is discussed.

A. Design Logic of the Proposed Neighbor Discovery Protocol

In lower frequency communication networks, where omnidirectional antennas are equipped on transmitters and receivers, the received signal strength P_{rx}, which indicates both the direction of the signal source corresponding to the receiver's coordinate and the distance between the signal source and the receiver, can be used as a crucial data in the neighbor discovery process. However, in THz communication networks, P_{rx}, as aforementioned in Sec. II, is not only a function of distance r, but also affected by the time t, the initial angles $\theta_{tx}^{int}, \theta_{rx}^{int}$ and the turning speeds ω_{tx}, ω_{rx} of the transmitter and receiver, respectively. Different combinations of aforementioned factors can lead to the same P_{rx} value. Thus, it is not possible to locate the signal source by just using P_{rx} without knowing the detailed combination of all the factors. An universal standard to fast locate the signal source with only limited information of the received signal samples is highly needed.

Fortunately, during the turning of the transmitter and receiver DAs, the changing rate of the total antenna gain, $\Delta G(t)/\Delta t$, shows a certain data pattern, which is not affected by the change of the transmitter's location and periodically repeats itself. $G(t)$ refers to the total DAs' gain, which can be derived with a series of continuously received signal samples. In this case, as long as the receiver receives several continuous signal samples from a specific transmitter, it can map the received signal information to the $\Delta G(t)/\Delta t$ data pattern, and then, find the matched direction of the specific transmitter.

B. Process of Neighbor Discovery with Side-lobe Information

As shown in Fig. 3, the simplest scenario is tested between one transmitter and one receiver which are configured as follows: the transmitter's DA always points to the receiver, and the receiver's DA turns in a constant speed of 2ω and direction, which, in the perspective of detecting the data pattern from the received signal samples, is equivalent to the scenario that both transmitter's DA and receiver's DA turning in constant speeds of ω with different directions. The changing rate of the received signal samples is symmetrical about the origin direction of the receiver, which is pointing towards the transmitter, and gets extremely weak after the main-lobe of the receiver's DA passes certain angle away from the origin direction. Thus, we analyze the $\Delta G(t)/\Delta t$ data pattern within a certain angle range of the receiver DA's main-lobe, from 0 to $\pi/2$. In order to observe more distinguished differences in the data pattern, we utilize the equivalent changing rate of the electric-field intensity of the antenna, noted as $\Delta E(t)/\Delta t$, for data pattern analysis, where $G(t) = 20\log_{10}E(t)$. All data patterns shown in Fig. 3 are derived from the 10×10-elements planar array.

The first derivative of the $E(t)$ is shown in Fig. 3a, from which we observe that, the data pattern of $\Delta E(t)/\Delta t$ fluctuates over the passed angle of the receiver DA's main-lobe, and progressively becomes weak as the main-lobe of the receiver DA turns away from the origin direction. The difficulty of neighbor detection by using $\Delta E(t)/\Delta t$ data pattern is that, any coming $\Delta E(t)/\Delta t$ data sample can be mapped to n potential directions, giving that $n \geq 2$. To detect the potential direction in the green-shaded region, we need at least two continuous data samples, which is enough due to the opposite trends of data samples' changing rate, i.e., increase and decrease, which guarantees the 1 to 1 mapping between the received data samples and the potential direction of the neighbor. For the pink-shaded region where more uncertainty exists due to the 1 to n mapping, an additional assisted $d^2E(t)/dt^2$ data pattern needs to be taken into consideration. The bottom part of Fig. 3a shows the $d^2E(t)/dt^2$ data pattern, which is calculated based on the same scenario, the positive sharp pulses in the $d^2E(t)/dt^2$ data pattern indicate the drastically increasing parts in $\Delta E(t)/\Delta t$ data pattern. In this case, we can detect the potential directions corresponding to b, d, f and h by different amplitude of the positive pulses from the $d^2E(t)/dt^2$ data pattern.

As presented in Fig. 3b, the zoomed-in plot of the negative parts of $d^2E(t)/dt^2$ data pattern correlate with the decreasing parts in $\Delta E(t)/\Delta t$ data pattern, which to some extent overlaps with each other. The corresponding parts between two data patterns are marked by yellow-shaded boxes, within which we observe that the fractions of a, c^1, c^2, e^1, g^1 and i^1 in the $d^2E(t)/dt^2$ data pattern have 1-to-1 mapping property between the received data samples $d^2E(t)/dt^2$ and the potential directions of neighbors, thus, can be leveraged in neighbor discovery. However, the other parts in the $d^2E(t)/dt^2$ data pattern more or less overlap with each other, thus, cannot be used for direction detection of the signal source.

Another additional assisted data pattern, which is derived by taking the third derivative of $E(t)$ is presented in Fig. 3c. Now, only those undetermined parts in $d^2E(t)/dt^2$ data pattern need further detections. The correlated parts of most undetermined fractions in $d^3E(t)/dt^3$ data pattern have 1 to 1 mapping property in light of either increasing changing rate of $d^3E(t)/dt^3$, e.g., e^2, g^2 and i^2, or decreasing changing
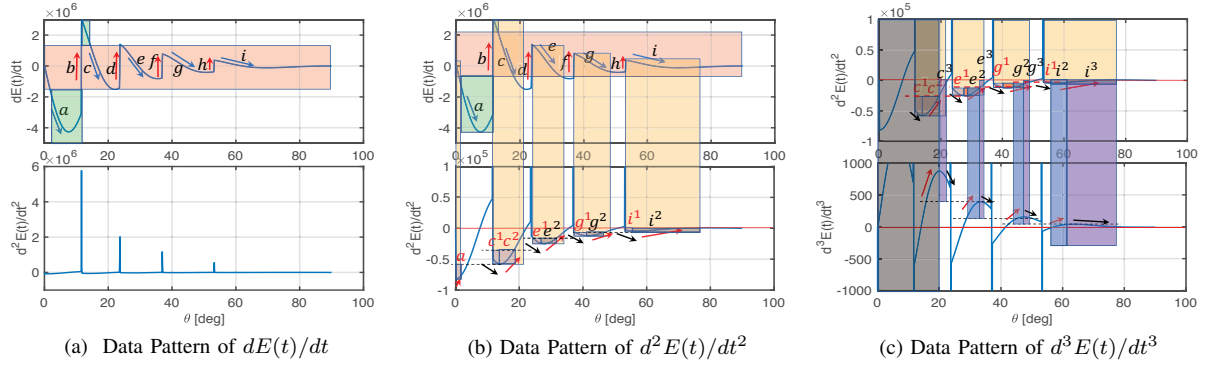
Fig. 3: Impact of side-lobe information in neighbor discovery

rate of $d^3E(t)/dt^3$, e.g., c^3, e^3, g^3 and i^3. In this case, the vast majority of the potential directions can be accurately detected with the cooperation of aforementioned three data patterns, for the rest of uncertain potential directions, we can either apply a higher order derivative function of $E(t)$ to assist in neighbor discovery or map the rest of uncertain potential directions from $d^2E(t)/dt^2$ data pattern, which have distinct differences as shown with the very small red-shaded blocks. For different scenarios, the selection is depends on the weight of the uncertain parts.

IV. PROTOCOL COMPARISION

In this section, we mathematically analyze and compare the performance of two different neighbor discovery protocols, i.e., without and with side-lobe information. The latter is based on the analysis provided in Sec. III. We first focus on the analysis of the discovery of a single node, then we extend our analysis to the process of discovering all one-hop neighbors of the receiver. During this process, we consider the randomness of the network topology and the turning property of the nodes' DAs as we introduced in Sec. II.

A. Neighbor Discovery without Side-lobe Information

This protocol only considers the complete alignment and facing of main-lobes of both transmitter and receiver DAs to be the sufficient condition of effective neighbor discovery. We define a random variable $X(\theta_{tx}^{int}, \theta_{rx}^{int}, t)$ to represent the discovery process of the turning DAs of both transmitter and receiver and express the random variable as:

$$X(\theta_{tx}^{int}, \theta_{rx}^{int}, t) = g(\theta_{tx}^{int} + \omega_{tx}t)g(\theta_{rx}^{int} + \omega_{rx}t), \quad (6)$$

where the initial angles of the transmitter DA and receiver DA are measured as the angles pass away from the original angle direction which is facing towards each other. Besides, the turning speed in this function has the property of turning direction.

With aforementioned information, the probability for RX to discover one specific TX_0 is calculated by satisfying the condition that the random variable $X(\theta_{tx}^{int}, \theta_{rx}^{int}, t) == 1$. $\theta_{tx}^{int}, \theta_{rx}^{int}$ and t are all uniform distributed variables on angle range $[-\pi, \pi]$ and time duration $[0, T]$ respectively. The p.d.f

of $\theta_{rx}^{int}, \theta_{tx}^{int}$ are $1/2\pi$, the p.d.f of t is $1/T$. The probability for RX to find the specific TX_0 is given by:

$$P_{find}^{one} = \int_{t=0}^{T} \int_{\theta_{rx}^{int}=-\pi}^{\pi} \int_{\theta_{tx}^{int}=-\pi}^{\pi} \mathbf{1}\left(X(\theta_{tx}^{int}, \theta_{rx}^{int}, t) == 1\right)$$
$$\frac{1}{4\pi^2}\frac{1}{T}d\theta_{rx}^{int}d\theta_{tx}^{int}dt = \frac{E\left[T_{find}^{one}\right]}{T},$$
(7)

where $\mathbf{1}(\cdot)$ is the indicator function which takes the value 1 when the argument is true, and takes 0 otherwise. $E\left[T_{find}^{one}\right]$ is the expected time for RX to discover the specific TX_0, which can be calculated by multiplying T on both sides of (7).

Since the neighbor discovery process of each node is independent, and we consider that RX cannot discover several TXs simultaneously within one sector time, which, to keep DA's fast turning speed, is designed for one successful packet transmission and reception. Thus, the expected time of discovering all TXs that locating within A of RX is calculated as:

$$E\left[T_{find}^{all}\right] = \sum_{i=1}^{N_t} P_{find}^{one}E\left[T_{find}^{one}\right] = N_t P_{find}^{one}E\left[T_{find}^{one}\right]. \quad (8)$$

B. Neighbor Discovery with Side-lobe Information

As we introduced in Sec. III, as long as the receiver successfully receives enough continuous signal samples from the specific neighbor, it will be able to map the received signals to the data patterns and to locate the specific neighbor. The issue in this scenario is that the receiver may not be able to detect the specific neighbor immediately, even if they are located close to each other. This problem is caused by the instantaneous signal to interference ratio (SIR) detected by, for example, the side-lobes of the receiver antenna, which may not be sufficient to surpass the SIR threshold β. Our proposed method only take those continuous signals, whose power strength surpass β as effective signals to accomplish the neighbor discovery process.

Assuming that RX is in the process of discovering one specific neighbor TX_0, who locates r_0 away from RX, the

received signal power at RX is calculated as:

$$P_{rx}^0(r_0, \theta_{tx_0}^{int}, \theta_{rx_0}^{int}, t) = \gamma g(\theta_{tx_0}^{int} + \omega_{tx}t)g(\theta_{rx_0}^{int} + \omega_{rx}t)r_0^{-2}e^{-Kr_0}, \quad (9)$$

The interference created by any other neighbor, e.g., TX_i, located within A and at a distance of r_i with RX, is calculated as:

$$I(r_i, \theta_{tx_i}^{int}, \theta_{rx_i}^{int}, t) = \gamma g(\theta_{tx_i}^{int} + \omega_{tx}t)g(\theta_{rx_i}^{int} + \omega_{rx}t)r_i^{-2}e^{-Kr_i} \quad (10)$$

We consider that TX_i is uniformly distributed within the one hop coverage area of RX. The c.d.f of r_i is calculated as:

$$F_X(r_i) = \frac{\pi r_i^2}{\pi R^2} = \frac{r_i^2}{R^2}, \quad (11)$$

thus, the p.d.f of r_i is $\frac{2r_i}{R^2}$. Considering that each node is independent with others, the expected value of interference caused by all the rest neighbors is given by:

$$E(I) = (N_t - 1)\int_{t=0}^{T}\int_{\theta_{tx_i}^{int}=-\pi}^{\pi}\int_{\theta_{rx_i}^{int}=-\pi}^{\pi}\int_{r_i=0}^{R} I(r_i, \theta_{tx_i}^{int}, \theta_{rx_i}^{int}, t)\frac{2r_i}{R^2}\frac{1}{4\pi^2}\frac{1}{T}dr_i d\theta_{rx_i}^{int}d\theta_{tx_i}^{int}dt. \quad (12)$$

For any pair of the discovering node and one specific neighbor, the SIR is calculated as:

$$S(r_0, \theta_{tx_0}^{int}, \theta_{rx_0}^{int}, t) = P_{rx}^0(r_0, \theta_{tx_0}^{int}, \theta_{rx_0}^{int}, t)E\left[\frac{1}{I}\right], \quad (13)$$

where $E[\frac{1}{I}] \neq \frac{1}{E[I]}$, and $E[\frac{1}{I}]$ is calculated as [9]:

$$E\left[\frac{1}{I}\right] = g(\mu_0) + \frac{g''(\mu_0)}{2}\sigma^2[I], \quad (14)$$

where μ_0 is the mean value of random variable I, $\mu_0 = E[I]$ and $g(\mu_0) = \frac{1}{\mu_0} = \frac{1}{E[I]}$, then we can calculate $g''(\mu_0) = \frac{2}{\mu_0^3} = \frac{2}{(E[I])^3}$, $\sigma^2[I]$ is the variance of I which can be calculated as $\sigma^2[I] = E[I^2] - (E[I])^2$. After simplification, (14) can be rewriten as:

$$E\left[\frac{1}{I}\right] = \frac{E[I^2]}{(E[I])^3}, \quad (15)$$

the calculation of $E[I^2]$ is expressed as:

$$E[I^2] = (N_t - 1)\int_{t=0}^{T}\int_{\theta_{rx_i}^{int}=-\pi}^{\pi}\int_{\theta_{tx_i}^{int}=-\pi}^{\pi}\int_{r_i=0}^{R} I^2(r_i, \theta_{tx_i}^{int}, \theta_{rx_i}^{int}, t)\frac{2r_i}{R^2}\frac{1}{4\pi^2}\frac{1}{T}dr_i d\theta_{rx_i}^{int}d\theta_{tx_i}^{int}dt \quad (16)$$

Suffering the interference created by all surrounding TX_i, the probability that RX discovers one specific TX_0 by receiving effective signal samples is calculated as:

$$P_{find}^{one} = \int_{t=0}^{T}\int_{\theta_{rx_0}^{int}=-\pi}^{\pi}\int_{\theta_{tx_0}^{int}=-\pi}^{\pi}\int_{r_0=0}^{R} \mathbf{1}\left(S(r_0, \theta_{tx_0}^{int}, \theta_{rx_0}^{int}, t) \geq \beta\right)\frac{2r_0}{R^2}\frac{1}{4\pi^2}\frac{1}{T}dr_0 d\theta_{rx_0}^{int}d\theta_{tx_0}^{int}dt, \quad (17)$$

The total time needed to discover all the neighbors located within the one hop coverage area of the receiver is calculated as:

$$E[T_{find}^{all}] = \sum_{i=1}^{N_t}P_{find}^{one}(N_s\Delta t) = N_t P_{find}^{one}(N_s\Delta t), \quad (18)$$

where N_s is the number of the continuously received effective signal samples that are utilized to achieve the neighbor discovery process. In the case of applying 3 data patterns to form the neighbor discovery standard, $N_s = 5$, which is calculated by converting the number of received data samples from the highest order derivative of $E(t)$ down to the $E(t)$. $1/\Delta t$ refers to the received signal sample rate. In this paper, we test with the slowest sample rate by considering the antenna turning in a sector by sector pattern, thus:

$$\Delta t = \frac{\min(\theta_{sec}^{tx}, \theta_{sec}^{rx})}{|\omega_{rx} - \omega_{tx}|}, \quad (19)$$

where θ_{sec}^{tx} and θ_{sec}^{rx} stand for one sector angle of transmitter DA and receiver DA perspectively.

V. Numerical Results

In this section, unless otherwise stated, we consider a network as introduced above with the following system parameters: the central frequency f_0 is $1.03\ THz$, the maximum radius R of one hop coverage area of the receiver is $10\ m$, the transmission power P_{tx} is $-20\ dBm$, the number of elements N of antenna array is 10, the maximum power pattern G_{max} of the antennas is $40\ dB$, the SIR threshold β is $10\ dB$. the transmitter and receiver DAs turn in the same speed but with opposite directions. We consider a constant background noise equals $-110\ dBm$ in addition to the interference created by side-lobes.
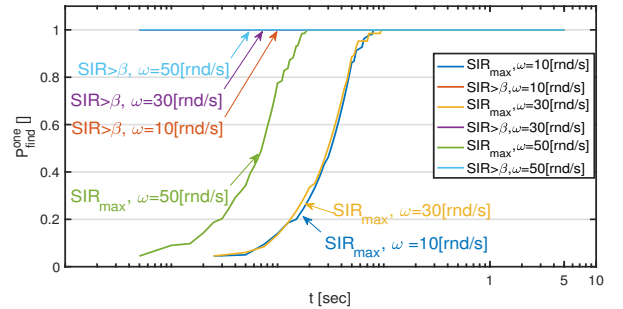

Fig. 4: Comparison of neighbor discovery protocols for a single neighbor

As shown in Fig. 4, we test the performance of finding a specific neighbor of the discovering node with different neighbor discovery protocols, i.e., with and without side-lobes, indicated as $SIR > \beta$ and SIR_{max}, respectively. Since the neighbor discovery protocol without side-lobes requires complete alignment and facing of the transmitter's main-lobe and receiver's main-lobe. The probability of finding the specific neighbor increases slowly with time, before the discovering node completely finds the specific neighbor, i.e., when P_{find}^{one}

approach to 1, it already consumed more time than that of our proposed protocol. Comparatively, the proposed neighbor discovery protocol removes the limitation of utilizing side-lobes, as long as the received SIR surpasses the β, the effective signal is successfully received and assisted in neighbor detection. Thanks to the participation of side-lobes, the discovering node find the specific neighbor almost immediately. Also, faster DAs' turning speeds accelerate the neighbor discovery process, and thus, cause P_{find}^{one} to approach to 1 faster. Because of the difficulty to achieve infinite small time steps, it's easy to skip the effective facing factor combinations under the strict facing rule, i.e., the protocol without side-lobes. Thus, randomness is involved in the calculation of P_{find}^{one}, however, it doesn't change the trend of the result.
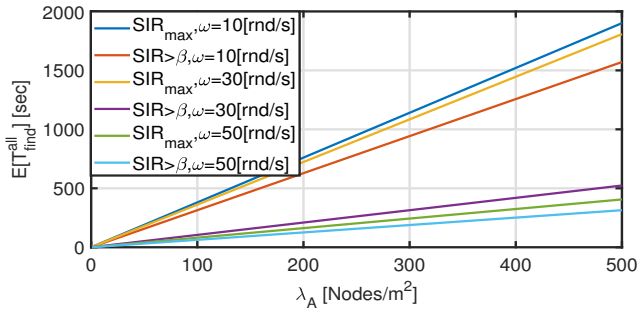

Fig. 5: Expected time needed to discover all neighbors

The total time consumption of discovering all surrounding neighbors of the discovering node is presented in Fig. 5, in which we compares the aforementioned two neighbor discovery protocols with different neighbor densities and DAs' turning speeds. It can be seen from the results that, faster turning speeds of transmitters' DAs and receivers' DAs help to speed up the neighbor discovery process for both protocols. When neighbor density increases, both neighbor discovery protocols take more time for the discovering node to detect its neighbors. In general, the protocol that captures the information of side-lobes performs better than the protocol without side-lobes.
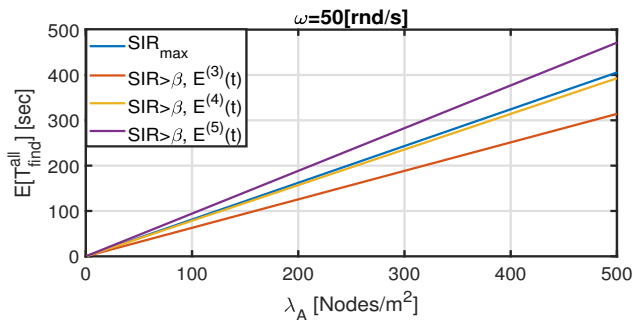

Fig. 6: Expected time needed to discover all neighbors with more data patterns

As shown in Fig. 6, there exist the boundary of applying the highest order of data pattern, the highest order of data pattern suitable for the 10×10-elements planner array studied in this paper is up to the fourth order of derivative function of

$E(t)$. The proposed neighbor discovery protocol will loss the advantage comparing with the protocol without side-lobes by taking $d^5 E(t)/dt^5$ into consideration.

VI. CONCLUSION

In this paper, an expedited neighbor discovery protocol that leverages antenna side-lobe information has been proposed based on the unique peculiarities of THz-band communication. The location mapping scheme for the received signal samples has been devised and analyzed. A comparison between our proposed protocol and the protocol without side-lobes has been mathematically analyzed and derived, based on which, the numerical results have been provided to illustrate the improvement of our proposed neighbor discovery protocol.

REFERENCES

[1] Cisco visual networking index: Global mobile data traffic forecast update, 20162021 white paper.

[2] I. F. Akyildiz, J. M. Jornet, and C. Han, "Terahertz band: Next frontier for wireless communications," *Physical Communication*, vol. 12, pp. 16–32, 2014.

[3] T. Kurner and S. Priebe, "Towards THz Communications-Status in Research, Standardization and Regulation," *Journal of Infrared, Millimeter, and Terahertz Waves*, vol. 35, no. 1, pp. 53–62, 2014.

[4] J. M. Jornet and I. F. Akyildiz, "Channel modeling and capacity analysis of electromagnetic wireless nanonetworks in the terahertz band," *IEEE Transactions on Wireless Communications*, vol. 10, no. 10, pp. 3211–3221, Oct. 2011.

[5] S. Priebe and T. Kurner, "Stochastic modeling of thz indoor radio channels," *IEEE Transactions on Wireless Communications*, vol. 12, no. 9, pp. 4445–4455, 2013.

[6] V. Radisic, K. Leong, D. Scott, C. Monier, X. Mei, W. Deal, and A. Gutierrez-Aitken, "Sub-millimeter wave InP technologies and integration techniques," in *IEEE MTT-S International Microwave Symposium (IMS)*, May 2015, pp. 1–4.

[7] S. Slivken and M. Razeghi, "High power, electrically tunable quantum cascade lasers," in *SPIE OPTO*. International Society for Optics and Photonics, 2016, pp. 97 550C–97 550C.

[8] Q. Xia, Z. Hossain, M. Medley, and J. M. Jornet, "A link-layer synchronization and medium access control protocol for terahertz-band communication networks," in *2015 IEEE Global Communications Conference (GLOBECOM)*, Dec 2015, pp. 1–7.

[9] V. Petrov, M. Komarov, D. Moltchanov, J. M. Jornet, and Y. Koucheryavy, "Interference and sinr in millimeter wave and terahertz communication systems with blocking and directional antennas," *IEEE Transactions on Wireless Communications*, vol. 16, no. 3, pp. 1791–1808, March 2017.

[10] X.-W. Yao, C.-C. Wang, W.-L. Wang, and C. Han, "Stochastic geometry analysis of interference and coverage in terahertz networks," *Nano Communication Networks*, vol. 13, no. Supplement C, pp. 9 – 19, 2017.

[11] J. Kokkoniemi, J. Lehtomki, and M. Juntti, "Stochastic geometry analysis for mean interference power and outage probability in thz networks," *IEEE Transactions on Wireless Communications*, vol. 16, no. 5, pp. 3017–3028, May 2017.

[12] S. Singh, R. Mudumbai, and U. Madhow, "Interference analysis for highly directional 60-ghz mesh networks: The case for rethinking medium access control," *IEEE/ACM Trans. Netw.*, vol. 19, no. 5, pp. 1513–1527, Oct. 2011.

[13] C. A. Balanis, *Antenna Theory: Analysis and Design*. Wiley-Interscience, 2005.